



Published in final edited form as:

Arterioscler Thromb Vasc Biol. 2019 September ; 39(9): 1747–1761. doi:10.1161/ATVBAHA.119.312382.

Targeted deletion of hepatocyte *Abca1* increases plasma HDL reverse cholesterol transport via the LDL receptor

Alexander C. Bashore, PhD¹, Mingxia Liu, PhD¹, Chia-Chi C. Key, PhD¹, Elena Boudyguina, PharmD¹, Xianfeng Wang, PhD¹, Caitlin M. Carroll, BA³, Janet K. Sawyer, MS¹, Adam E. Mullick, PhD², Richard G. Lee, PhD², Shannon L. Macauley, PhD³, John S. Parks, PhD¹

¹Department of Internal Medicine, Section on Molecular Medicine, Wake Forest School of Medicine, Winston-Salem, NC 27157

²Cardiovascular Group, Antisense Drug Discovery, Ionis Pharmaceuticals, Inc., Carlsbad, CA 92010, USA.

³Department of Internal Medicine, Section on Gerontology and Geriatric Medicine, Wake Forest School of Medicine, Winston-Salem, NC 27157

Abstract

Objective—The role of hepatocyte ATP binding cassette transporter A1 (*Abca1*) in trafficking hepatic free cholesterol (FC) into plasma versus bile for reverse cholesterol transport (RCT) is poorly understood. We hypothesized that hepatocyte *Abca1* recycles plasma HDL cholesterol (HDL-C) taken up by the liver back into plasma, maintaining the plasma HDL-C pool and decreasing HDL-mediated RCT into feces.

Approach and Results—Chow-fed hepatocyte-specific *Abca1* knockout (HSKO) and control mice were injected with human HDL radiolabeled with ¹²⁵I-tyramine cellobiose (¹²⁵I-TC;protein) and ³H-cholesteryl oleate (³H-CO). ¹²⁵I-TC and ³H-CO plasma decay, plasma HDL ³H-CO selective clearance (i.e., ³H-¹²⁵I fractional catabolic rate), liver radiolabel uptake, and fecal ³H-sterol were significantly greater in HSKO versus control mice, supporting increased plasma HDL RCT. Twenty-four hours after ³H-CO-HDL injection, HSKO mice had reduced total hepatic ³H-FC (i.e., ³H-CO hydrolyzed to ³H-FC in liver) resecretion into plasma, demonstrating *Abca1* recycled HDL-derived hepatic ³H-FC back into plasma. Despite similar liver LDL receptor (LDLr) expression between genotypes, HSKO mice treated with LDLr-targeting versus control antisense oligonucleotide had slower plasma ³H-CO-HDL decay, reduced selective ³H-CO clearance, and decreased fecal ³H-sterol excretion that were indistinguishable from control mice. Increased RCT in HSKO mice was selective for ³H-CO-HDL, since macrophage RCT was similar between genotypes.

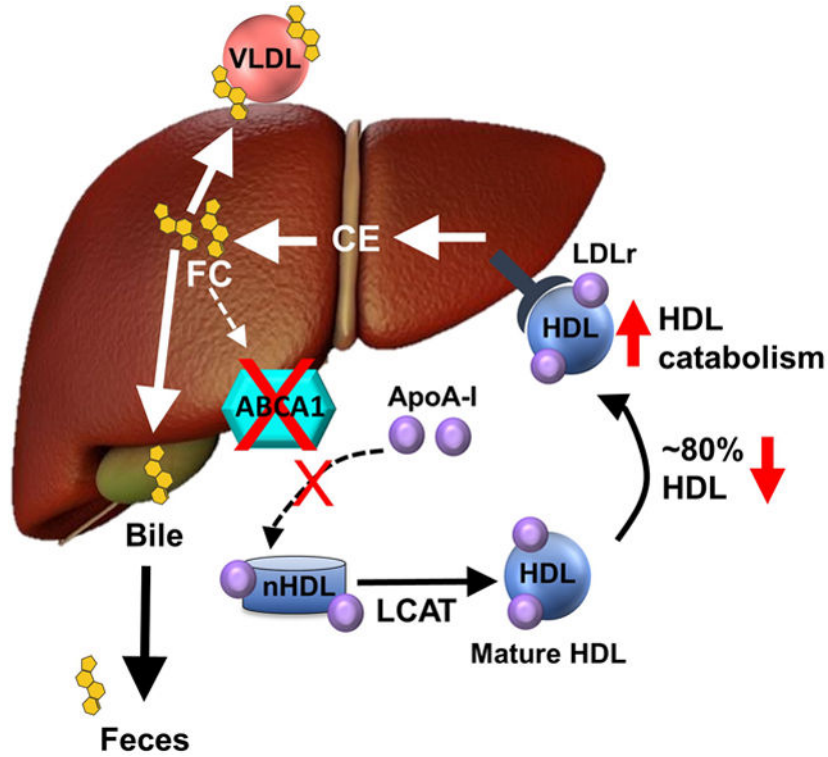
Conclusions—Hepatocyte *Abca1* deletion unmasks a novel and selective FC trafficking pathway that requires LDLr expression, accelerating plasma HDL-selective CE uptake by the liver

To whom correspondence should be addressed: Dr. John S. Parks, Department of Internal Medicine/Section of Molecular Medicine, Wake Forest School of Medicine, Medical Center Blvd., Winston-Salem, NC 27157, USA. jparks@wakehealth.edu Tel: +1 336 716 2145; Fax: +1 336 716 6279.

Disclosures: Drs. Mullick and Lee are employees of Ionis Pharmaceuticals, Inc. All other authors have no conflicts of interest.

and promoting HDL RCT into feces, consequently reducing HDL-derived hepatic FC recycling into plasma.

Graphical Abstract



Keywords

Abca1; High Density Lipoproteins; Cholesterol; Lipoproteins/Kinetics; Liver Metabolism

Subject terms

Lipids and Cholesterol; Metabolism

Introduction

Coronary heart disease (CHD) remains the leading cause of death worldwide. Statins, which reduce circulating plasma low density lipoprotein (LDL) concentrations, have lowered mortality attributable to CHD ¹, yet CHD risk remains in statin-treated individuals ². Epidemiologic studies have documented a strong inverse association between plasma high density lipoprotein cholesterol (HDL-C) concentrations and CHD, suggesting that HDL is an anti-atherogenic lipoprotein ³⁻⁵. However, treatments to raise plasma HDL concentrations and reduce CHD risk have had limited success ⁶⁻⁸. HDL’s atheroprotective role is attributed to its participation in reverse cholesterol transport (RCT), where HDL mobilizes extrahepatic cholesterol, particularly from arterial macrophage foam cells, and transports it to the liver for bile secretion and fecal excretion ⁹. HDL cholesterol efflux capacity measures

the ability of plasma HDL (i.e., apoB lipoprotein deleted plasma or serum) to accept cellular free cholesterol, the first step in the biogenesis of HDL and RCT. HDL cholesterol efflux capacity better predicts CHD risk than plasma HDL-C concentrations^{10, 11}.

HDL biogenesis is initiated via ATP binding cassette transporter A1 (ABCA1), a cellular plasma membrane cholesterol and phospholipid efflux protein that assembles effluxed cellular lipids with apolipoproteins, such as apolipoprotein A-I and E, forming nascent HDL particles¹²⁻¹⁴. Although ABCA1 is expressed throughout the body, hepatocyte ABCA1 expression is largely responsible for maintaining plasma HDL-C levels¹⁴. Mutations that inactivate *ABCA1* lead to Tangier disease, a disorder characterized by near-absence of plasma HDL, increased extra-hepatic tissue cholesterol accumulation, decreased plasma LDL concentrations, and increased plasma TG levels¹⁵⁻¹⁷. Studies using hepatocyte-specific *Abca1* knockout (HSKO) mice have shown that the Tangier disease plasma lipid and lipoprotein phenotype can be explained almost entirely by loss of hepatocyte *Abca1* activity¹⁸, except for ~20–30% of plasma HDL generated by the intestine and adipose tissue^{19, 20}. This marked reduction of plasma HDL-C is due to defective assembly of nascent HDL by hepatocytes and increased plasma clearance of HDL protein and cholesteryl ester (CE)^{14, 18, 21, 22}. Although our knowledge of hepatocyte *Abca1* in plasma lipoprotein formation and catabolism is growing, the role of *Abca1* in trafficking HDL-C taken up by the liver into the RCT pathway is less clear.

Recently, Yamamoto et al.²³ demonstrated that mice fed probucol, an *Abca1* inhibitor, had increased plasma HDL RCT into feces, despite ~80% lower plasma HDL-C. This suggests that without hepatic *Abca1* activity, plasma HDL-C taken up by the liver is preferentially trafficked into the RCT pathway for biliary secretion and fecal excretion, not resecreted into plasma. However, probucol has pleotropic effects and is not a specific hepatocyte *Abca1* inhibitor^{24, 25}. Furthermore, direct evidence that *Abca1* recycles plasma HDL-derived hepatic FC is lacking, indicating significant gaps in knowledge about hepatocyte *Abca1* in HDL-C RCT.

The current study was designed to investigate the role of hepatocyte *Abca1* in plasma HDL RCT and recycling of hepatic cholesterol into plasma. We hypothesized that hepatocyte *Abca1* recycles a significant amount of plasma HDL-C, taken up by the liver, back into plasma, maintaining the plasma HDL-C pool and decreasing HDL-mediated RCT into feces. Our results demonstrate that hepatocyte *Abca1* is pivotal in resecretory plasma-derived HDL-C back into plasma versus trafficking into RCT excretion pathways and reveal a novel role for the hepatic LDL receptor (LDLr) in stimulating plasma HDL selective CE uptake and trafficking of sterol into RCT when hepatocyte *Abca1* is absent. Our data also suggest that hepatocyte *Abca1* inhibition or haploinsufficiency due to coding variants may promote HDL RCT in parallel with a significant reduction in plasma HDL-C.

Materials and Methods

(please see the Major Resources Table in the Supplemental Material for reagent details)

Animals

For each experiment, chow-fed age-matched 12- to 24-week-old male and female *Abca1^{flox/flox}* or C57BL/6J (The Jackson Laboratory; Stock # 000664) mice (controls) and hepatocyte-specific *Abca1* knockout (HSKO) mice were used. HSKO mice were generated by crossing *Abca1^{flox/flox}* mice¹⁴ (backcrossed >99% into the C57BL/6 background) with albumin *Cre* recombinase transgenic mice (The Jackson Laboratory; Stock # 003574). All mice were maintained in a specific pathogen-free environment on a 12:12 h light:dark cycle (dark cycle, 6 p.m. to 6 a.m.) and allowed free access to standard chow diet (Purina – LabDiet; Prolab RMH 3000) and water. Cage bedding was Bed-o’Cobs (1/8”) from Andersons Lab Bedding and mice were provided with EnviroPak for enrichment (W.F. Fisher & Son, Inc.). Mouse studies were performed in facilities approved by the American Association for Accreditation of Laboratory Animal Care using a protocol approved by the Institutional Animal Care and Use Committee at Wake Forest School of Medicine.

Lipoprotein Preparation and Radiolabeling

Pooled human plasma was obtained from the American Red Cross and mouse plasma was obtained via cardiac puncture from C57BL/6J mice. HDL (d=1.063–1.21 g/mL) was isolated from plasma by sequential density ultracentrifugation²⁶.

HDL was radiolabeled with ³H-cholesteryl oleate (³H-CO) (Perkin Elmer) using human lipoprotein-deficient serum (LPDS) as a source of cholesteryl ester transfer protein²⁷. HDL protein was radiolabeled using ¹²⁵I-tyramine cellobiose (¹²⁵I-TC) (Perkin Elmer) according to methods previously described^{28, 29}.

HDL Turnover Studies

Control and HSKO mice were anesthetized with isoflurane and intravenously (retroorbital) injected with ¹²⁵I-TC (0.1–0.3×10⁶ cpm; 50 cpm/ng HDL protein) and ³H-CO-HDL (0.5–1×10⁶ dpm; 200 dpm/ng HDL CE) tracers. Blood samples were taken 2 minutes, 30 minutes, 1, 3, 5, 8, 24, and 48 hours after tracer injection and experiments terminated at 24 or 48 hours. Plasma samples were directly quantified for ¹²⁵I-TC protein radiolabel using a gamma counter, or lipid extracted³⁰ to quantify ³H radiolabel using a liquid scintillation counter. Plasma HDL turnover curves were generated by plotting the percentage of the two-minute radiolabel remaining in plasma at each time point. The total amount of plasma radiolabel at each time point was determined by multiplying the ¹²⁵I cpm/ml or ³H dpm/ml plasma by total plasma volume, estimated as 3.5% of body weight. Fractional catabolic rates (FCR) were calculated by using SigmaPlot software to fit curves to a double exponential decay curve with 4 parameters ($y=ae^{-bx}+ce^{-dx}$), as previously described³¹.

Liver, kidney, and feces were collected at completion of each turnover study. ¹²⁵I-TC tissue uptake was measured by quantifying ¹²⁵I radiolabel in 50–100 mg of tissue using a gamma counter. To quantify ³H tissue uptake and fecal excretion, tissue and feces were lipid extracted and ³H was quantified by liquid scintillation counting^{32, 33}. Selective HDL ³H-CO removal from plasma was calculated as ³H FCR-¹²⁵I FCR³⁴. To determine the role of liver LDLr in HDL turnover, control and HSKO mice were randomly assigned to received intraperitoneal injections of either LDLr targeting antisense oligonucleotides (ASO) (Ionis

Pharmaceuticals, Inc; ION 713852) or control ASO (ION 740133) at 5 mg/kg/week for 4 weeks. HDL turnover studies were then performed over 48 hours as described above.

Hepatic Recycling of Plasma HDL $^3\text{H-CO}$

Control and HSKO mice were intravenously injected with $^3\text{H-CO}$ radiolabeled ($2-4 \times 10^6$ dpm) HDL and blood samples were taken at 2 minutes, 1, 3, 5, 8, and 24 hours as described above. Plasma was isolated from blood samples and FC and individual CE fatty acyl species were separated by HPLC as described previously³⁵ with minor modifications. Briefly, plasma was lipid extracted³⁰ and the extract was filtered ($0.22 \mu\text{m}$), dried under N_2 , reconstituted in $10 \mu\text{L}$ of tetrahydrofuran-acetonitrile 80:20 (v:v), and injected onto a reverse phase HPLC column ($250 \times 4.6\text{mm}$, Ultrasphere $5\mu\text{m}$ ODS column, Mac-Mod Analytical Inc.). FC and CEs were eluted from the column with a mobile phase of acetonitrile:isopropanol 50:50 (v:v) and fractions were collected every minute for 30 minutes (flow rate= 2 mL/min). Each fraction was transferred to a scintillation vial, the solvent evaporated under N_2 , and a scintillation cocktail was added before ^3H quantification by liquid scintillation counting³⁵. Radioactivity in FC and CE fractions at each time point of the turnover study was normalized to percentage of the two-minute plasma total radioactivity.

To determine ^3H radiolabel distribution among plasma lipoproteins, terminal plasma isolated from blood taken 24 hours after $^3\text{H-CO-HDL}$ tracer injection was fractionated by fast protein liquid chromatography (FPLC) using a Superose 6 column; fractions were collected every minute (0.4 mL/min). Radiolabel in the FPLC fractions was quantified by liquid scintillation counting and fractions corresponding to VLDL, LDL, and HDL, based on elution position, were pooled, lipid extracted, and fractionated into FC and CE fatty acyl species by reverse phase HPLC analysis as described above.

In Vivo Macrophage RCT

Macrophage RCT assays were conducted as described previously^{33, 36}. J774 macrophages were radiolabeled with ^3H -cholesterol and cholesterol-loaded with acetylated LDL. Five hundred μL of cell suspension containing $\sim 1 \times 10^7$ cells/mL and $\sim 4 \times 10^6$ dpm/mL was injected into the peritoneal cavity of recipient mice. Plasma samples were collected at 3, 6, 24, 48, 72, and 96 hours. Feces were collected continuously from 0–48 hours and 48–96 hours. At the termination of the study, liver was harvested and ^3H tracer in plasma, liver, and feces was quantified after lipid extraction and scintillation counting^{32, 33}. One hundred μL of pooled plasma from terminal blood draws were fractionated by FPLC to determine ^3H radiolabel distribution among lipoproteins.

Plasma Lipid and Lipoprotein Analysis

Plasma was collected by tail bleeding from mice fasted for 4 hours following 4 weeks of ASO treatment. Total plasma cholesterol (TPC) concentrations were determined by enzymatic assay³⁷. Cholesterol distribution among lipoproteins was quantified after fractionation of plasma by FPLC size-exclusion chromatography³⁶.

Quantitative RT-PCR

Total RNA was extracted from snap-frozen liver tissue using TRI-Reagent (Molecular Research Center, Inc). Target gene mRNA abundance was quantified by quantitative real-time PCR using Luna® Universal One-Step RT-qPCR Kit (NEB, E3005L). GAPDH mRNA abundance was used to correct the target gene expression data. Relative quantification was calculated using the comparative threshold formula³⁸. Primers used in this study were: GAPDH; TGTGTCCGTCGTGGATCTGA (forward), CCTGCTTACCACCTTCTTGAT (reverse); ABCA1: CGTTTCCGGGAAGTGTCCTA (forward), GCTAGAGATGACAAGGAGGATGGA (reverse); LDLR: AGGCTGTGGGCTCCATAG (forward), TCGGGTCCAGGGTCATCT (reverse); SR-BI: TCCCCATGAACTGTTCTGTGAA (forward), TGCCCGATGCCCTTGA (reverse).

Immunoblotting

Frozen liver (50–100 mg) was homogenized using a polytron-aggregate tissue homogenizer in RIPA buffer containing protease inhibitor cocktail (Roche 05892791001). Proteins were fractioned by 4–20% Criterion™ TGX™ precast gels (Bio-Rad; 5671094) and transferred to a PVDF membrane. Membranes were blocked with 5% nonfat dry milk in Tris-buffered saline + 1% tween 20 (TBST), incubated with primary antibody at 4°C overnight, washed three times with TBST, and then incubated with secondary antibody for 1 h at room temperature. Blots were incubated with SuperSignal West Pico chemiluminescence substrate (Pierce) and visualized with a Fujifilm LAS-3000 camera. Primary antibodies used for immunoblots included the following: Abca1 (custom mademade³⁹; 1:1000), SR-BI (Abcam; ab217318; 0.187 ug/mL), LDLr (gift from Dr. Joachim Herz; 1:1000), and GAPDH was used as a loading control (Santa Cruz; 32233; 0.02 ug/mL). Secondary antibodies used for immunoblots were HRP-conjugated anti-mouse (1:10,000) and anti-rabbit (GE Healthcare; 1:10,000). Band intensities were quantified using Image Studio Lite (LI-COR Biosciences).

Statistics

All data are presented as mean ± standard error of the mean (SEM). Data were tested for normality (Kolmogorov and Smirnov test) and equal variance (Bartlett or Brown-Forsythe test) using GraphPad prism 7 software. Statistical analyses were performed using an unpaired two-tailed Student's t-test, one-way ANOVA with Tukey's post hoc analysis, or repeated measures ANOVA. For the ASO studies in which the number of mice per group was too few to test for normality, the non-parametric Kruskal-Wallis test was used.

Results

Hepatocyte-specific Abca1 deletion accelerates HDL ¹²⁵I-TC tracer plasma decay and tissue uptake

A major goal of this study was to determine how hepatocyte Abca1 affects plasma HDL-C catabolism and RCT. We previously reported increased plasma clearance and kidney uptake of ¹²⁵I-TC radiolabeled mouse HDL in HSKO versus control mice; however, liver uptake of the mouse ¹²⁵I-TC HDL tracer was similar for both genotypes¹⁴. Because mouse HDL

particles are monodispersed, whereas human HDL particles are polydispersed⁴⁰, exhibiting distinct size subfractions, we used human HDL tracer for our turnover studies to capture the complexity of HDL-C catabolism that likely impacts RCT. Figure 1 summarizes plasma decay and tissue accumulation of ¹²⁵I-TC human HDL tracer for two independent 24- or 48-hour studies. Plasma decay of human HDL ¹²⁵I-TC protein was 2–3 fold greater in HSKO recipient mice than control mice (Fig. 1A, B). ¹²⁵I-TC human HDL tracer accumulation by liver (Fig. 1C) and kidney (Fig. 1D) was also significantly greater in HSKO compared to control mice. The apparent decrease in liver ¹²⁵I-TC accumulation at 48 versus 24 hours (Fig. 1C) was likely due to cellular release and urinary excretion of ¹²⁵I-TC (or free ¹²⁵I) that occurs during prolonged turnover studies⁴¹. When analyzed separately, ¹²⁵I-TC-HDL FCRs were similar for male and female recipient mice, indicating no sex-related differences in HDL protein turnover (data not shown).

Hepatocyte-specific Abca1 deletion accelerates HDL cholesteryl oleate plasma decay, selective CE clearance, and RCT

Next, we explored the role of hepatocyte Abca1 in plasma HDL-derived CE RCT. Once in the liver, HDL ³H-CO is hydrolyzed to ³H-FC, which can be 1) resecreted into plasma in very low density lipoprotein (VLDL) or HDL particles, 2) esterified by acyl:CoA cholesterol acyltransferase 2, forming CE that can be stored in lipid droplets, 3) secreted into bile as ³H-FC, or 4) converted to bile acid and secreted into bile. The latter two pathways increase RCT. We radiolabeled isolated human HDL particles with ³H-CO and injected them into control and HSKO mice to measure radiolabel plasma clearance, CE selective clearance (i.e., ³H-¹²⁵I FCR), liver radiolabel accumulation, and fecal radiolabel excretion. Plasma decay of HDL ³H-CO was markedly faster in HSKO versus control recipient mice in two turnover studies (Fig. 2A). Die-away curves for the two studies over the first 24 hours were remarkably similar. Plasma FCR (Fig. 2B) for the HDL ³H-CO was 5–7-fold greater in HSKO recipient mice compared with controls in both studies. Plasma HDL ³H-CO selective clearance, calculated as plasma HDL ³H-CO minus ¹²⁵I-TC HDL FCR (from Figure 1) was 10- to 20-fold greater in HSKO mice (Fig. 2C). Liver accumulation of the HDL ³H-CO tracer in HSKO mice (Fig. 2D) was 2-fold greater at 24 hours and 1.9-fold greater at 48 hours than in control mice, showing more rapid removal of tracer from plasma in HSKO mice. Seventy percent of the liver ³H radiolabel at the 24-hour time point was FC for both genotypes of mice (Supplemental Figure I), suggesting efficient and equivalent intrahepatic hydrolysis of plasma HDL-derived ³H-CO to ³H-FC. Plasma HDL ³H-radiolabel RCT was similar between genotypes in the 24-hour study, but 2-fold higher in HSKO recipient mice in the 48-hour study (Fig. 2E), indicating that plasma HDL RCT is increased in the absence of hepatocyte Abca1 expression 48 hours after ³H-CO HDL tracer injection.

Hepatocyte Abca1 recycles plasma HDL-derived cholesterol taken up by the liver into plasma

To determine whether hepatocyte Abca1 recycles plasma HDL-derived cholesterol taken up by the liver into plasma, we injected ³H-CO-radiolabeled human HDL into control and HSKO recipient mice, collected blood samples over 24 hours, and measured appearance of ³H-FC and individual ³H-CE fatty acyl species in plasma. Since *in vitro* incubations of HDL tracer with plasma demonstrated that ³H-CO remained associated with the HDL fraction and

that there was minimal ^3H -CO hydrolysis to ^3H -FC over 24 hours (Supplemental Figure IIA and B, respectively), plasma appearance of ^3H -FC and ^3H -CE fatty acyl species can only result from hepatic uptake of plasma HDL ^3H -CO, hydrolysis of ^3H -CO to ^3H -FC (see Supplemental Figure I), and resecretion into plasma as ^3H -FC or as ^3H -CE fatty acyl species, other than CO, generated by liver acyl CoA:cholesterol acyltransferase 2 (ACAT2)- or plasma lecithin:cholesterol acyl transferase (LCAT)-mediated esterification. HPLC separation of plasma lipid extracts (Fig. 3) showed that ^3H -CO radiolabel decreased more rapidly in HSKO recipient mice than control mice, in agreement with ^3H -CO die-away data in Figure 2. There was little detectable ^3H radiolabel in plasma other than CO before 24 hours (Fig. 3A-E). However, at the 24-hour time point, considerable ^3H radiolabel was in FC and CE fatty acyl species besides CO (Fig. 3F), such as cholesteryl docosahexaenoate (C22:6 n-3), cholesteryl arachidonate (C20:4), and cholesteryl linoleate (C18:2); less ^3H radiolabel was found in all fractions in HSKO compared to control plasma samples. This occurred despite more ^3H radiolabel in HSKO livers 24 hours after HDL tracer injection (Fig. 2D), suggesting markedly decreased resecretion of plasma HDL-derived hepatic ^3H cholesterol in HSKO mice.

At 24 hours, overall recycling of HDL-C taken up by the liver was decreased in HSKO mice (Fig. 4A). We fractionated the 24-hour terminal plasma samples by FPLC size exclusion chromatography to determine radiolabel distribution of FC and CE fatty acyl species among VLDL, LDL and HDL. HSKO plasma had an increased proportion of ^3H radiolabel distributed in VLDL and less HDL, with a small increase in LDL, compared with control plasma (Fig. 4B, C). There was a 5-fold increase in VLDL ^3H -FC in HSKO plasma compared to control (Fig. 4D), no difference in LDL ^3H -FC (Fig. 4E), and an 80% reduction in HDL ^3H -FC (Fig. 4F). Minimal ^3H radiolabel was found in VLDL CE species (Fig. 4D). The LDL fraction contained ^3H -CE fatty acyl species similarly distributed in HSKO and control plasma (Fig 4E). ^3H -CE fatty acyl species also appeared in the HDL fraction where the amount of radiolabel was less in HSKO versus control plasma (Fig. 4F). These combined results provide direct support for the concept that Abca1 recycles hepatic FC derived from plasma HDL CO uptake back into plasma.

Plasma HDL- ^3H -CO hypercatabolism and increased RCT in HSKO mice depend on hepatic LDLr expression

We hypothesized that rapid plasma removal of human HDL ^3H -CO in HSKO recipient mice was due to increased expression of hepatic SR-BI, which mediates CE-selective uptake from HDL⁴². However, we observed significantly decreased hepatic SR-BI protein expression in HSKO compared to control livers (Fig. 5A-B), whereas hepatic SR-BI mRNA expression was similar between the two genotypes (Fig. 5C), making it unlikely that SR-BI expression was directly responsible for HDL-CE hypercatabolism in HSKO mice. In a previous study, hepatic LDLr expression was increased nearly 2-fold in HSKO versus control mice¹⁸ and doubling hepatic LDLr expression decreases plasma HDL-C in chow-fed mice⁴³. We hypothesized that increased LDLr expression in HSKO mice led to HDL hypercatabolism. However, in contrast to our previous study¹⁸, we observed similar hepatic LDLr protein expression (Fig. 5A-B) and mRNA abundance (Fig. 5C) in HSKO vs. control liver.

Increased LDLr expression is associated with reduced plasma HDL-C concentrations in mice^{43, 44}. Although hepatic LDLr expression was similar for HSKO and control mice, hepatic LDLr surface expression or recycling may be increased in the absence of hepatocyte Abca1, leading to increased catabolism of plasma HDL. To investigate whether liver LDLr is involved in plasma HDL hypercatabolism in HSKO mice, we treated control and HSKO mice with a control ASO or LDLr-targeting ASO for 4 weeks. LDLr ASO treatment significantly increased plasma cholesterol concentrations in both strains relative to control ASO (Supplemental Figure IIIA). Most of the plasma cholesterol increase with LDLr ASO treatment was in the LDL fraction, as anticipated, but HDL-C was also considerably increased in LDLr ASO-treated HSKO mice versus control ASO-treated HSKO mice (Supplemental Figure IIIB). LDLr-targeting ASO treatment eliminated hepatic LDLr protein (Supplemental Figure IIIC-D) and reduced gene expression by ~75% (Supplemental Figure IIIE) relative to control ASO in both genotypes of mice. On the other hand, hepatic SR-BI protein and gene expression were unaffected by LDLr ASO treatment (Supplemental Figure IIIC-E). LDLr ASO treatment of HSKO mice normalized plasma HDL ¹²⁵I-TC die-way curves (Fig 6A) and FCR (Fig. 6B) to those of control mice treated with control or LDLr-targeting ASO. These results suggest that HDL protein (i.e., ¹²⁵I-TC) hypercatabolism in HSKO recipient mice depends on hepatic LDLr expression.

Next, we examined plasma HDL-CE metabolism in mice treated with control or LDLr ASO. Human HDL ³H-CO plasma decay (Fig. 7A) and FCR (Fig. 7B) in HSKO recipient mice treated with LDLr ASO was normalized to those of control recipient mice treated with either control or LDLr ASO. Plasma selective HDL ³H-CO removal in HSKO mice was also diminished to control levels with LDLr ASO treatment (Fig. 7C). Hepatic accumulation of ³H-radiolabel was higher in HSKO than control mice. Hepatic ³H radiolabel was similar in HSKO mice treated with LDLr ASO or control ASO (Fig. 7D). HSKO versus control mice treated with control ASO had significantly more fecal ³H-sterol excretion (Fig. 7E), similar to earlier results for untreated mice (Fig. 2E). Treatment of HSKO mice with LDLr ASO reduced fecal ³H-sterol excretion to levels indistinguishable from HSKO or control mice treated with control ASO. Similar trends occurred with fecal cholesterol and bile acid ³H-radiolabel (Fig. 7E).

Human HDL particles are polydispersed, with multiple size subfractions, whereas mouse HDL particles are monodispersed⁴⁰. To determine whether the more rapid turnover of plasma HDL tracer in HSKO depended on use of human HDL tracer particles, we isolated plasma HDL from C57Bl/6 donor mice, radiolabeled HDL with ¹²⁵I-TC or ³H-CO, and repeated the plasma turnover and RCT studies. Mouse HDL ¹²⁵I-TC displayed more rapid plasma decay and FCR in HSKO versus control recipient mice (Supplemental Figure IV), similar to results with human HDL ¹²⁵I-TC tracer (Figure 1); LDLr ASO treatment of recipient mice had minimal influence on HDL ¹²⁵I-TC catabolism (Supplemental Figure IV). Qualitatively similar results were obtained for plasma HDL ³H-CO decay, FCR, HDL ³H-CO selective clearance from plasma, hepatic accumulation, and fecal ³H radiolabel excretion (Supplemental Figure V; **panels A-E**) as with human HDL ³H-CO tracer (Figure 2) and LDLr ASO treatment of HSKO recipient mice normalized plasma decay, selective CE clearance, and RCT (Supplemental Figure V). These results support the conclusion that the

more rapid plasma HDL catabolism, increased selective HDL CE plasma clearance, and greater RCT in HSKO mice was independent of the source of HDL tracer.

Macrophage reverse cholesterol transport is unaffected by hepatocyte *Abca1* deletion

We previously reported that macrophage RCT is not compromised in hyperlipidemic HSKO mice (i.e., HSKO mice in the LDLrKO background fed an atherogenic diet) compared to controls³⁶. To determine whether macrophage RCT is intact in normolipidemic HSKO mice, chow-fed control and HSKO mice were injected in the peritoneal cavity with ³H-cholesterol-loaded J774 macrophages and appearance of ³H radiolabel in plasma, liver, and feces measured. HSKO plasma had markedly less ³H radiolabel appearance than control plasma during the 96-hour RCT experiment (Fig. 8A). In control plasma, ³H distribution was associated with HDL and to a lesser extent, LDL (Fig. 8B), similar to cholesterol mass distribution (Supplemental Figure IIIB), whereas ³H radiolabel in HSKO plasma was extremely low in HDL and LDL fractions. However, ³H radiolabel in liver (Fig. 8C) or feces (Fig. 8D) were similar between genotypes.

Discussion

Hepatocyte *Abca1* plays a key role in production and catabolism of all three major plasma lipoprotein classes (VLDL, LDL, and HDL) that contribute to cardiometabolic risk^{18, 22}. In addition, chow-fed HSKO mice closely phenocopy lipid and lipoprotein alterations in Tangier disease subjects, suggesting HSKO mice are ideal for investigating *in vivo* metabolic pathways impacted by diminished hepatocyte *Abca1* expression. Despite our current understanding of hepatocyte *Abca1* in plasma lipoprotein metabolism, we do not understand its involvement in hepatic FC trafficking into plasma versus bile and feces for RCT. Our current study addresses this gap in knowledge and contributes three novel findings. First, HSKO mice showed increased selective HDL-CE removal from plasma and preferential trafficking of plasma-derived HDL-C into feces, increasing HDL RCT, compared to control mice. Second, absence of hepatocyte *Abca1* expression diminishes overall recycling of plasma HDL-C, taken up by the liver, back into the plasma compartment, but increases the portion of resecreted FC in VLDL particles at the expense of HDL particles, thereby affecting quantity and compartmentalization of resecreted hepatic FC. These results suggest that hepatocyte *Abca1* is an important gatekeeper for regulating hepatic FC flux between the plasma compartment and bile. Finally, increased selective HDL-CE removal from plasma and trafficking into the RCT pathway in HSKO mice depends on hepatic LDLr expression, identifying a novel role for the LDLr in plasma HDL RCT. Thus, our data suggest that hepatocyte *Abca1* inhibition or haploinsufficiency due to coding variants may promote HDL-C RCT despite a concomitant reduction in plasma HDL.

Specific genetic deletion of hepatocyte *Abca1* results in diminished nascent HDL particle assembly²² and increased HDL protein and CE catabolism^{14, 21}, resulting in reduced plasma HDL-C concentrations in chow-fed HSKO versus control mice. However, trafficking of HDL ³H-CO tracer through the RCT pathway has not been investigated in HSKO mice. Sterol balance studies in whole body *Abca1* knockout mice have suggested either no effect⁴⁵ or increased fecal sterol excretion due to reduced intestinal cholesterol absorption⁴⁶.

However, the role of hepatocyte Abca1 in hepatic cholesterol trafficking is confounded in whole body Abca1 knockout mice because of Abca1's widespread and variable tissue and cell expression⁴⁷. Yamamoto et al²³ showed increased fecal excretion of plasma HDL-derived cholesterol in mice fed probucol, an Abca1 inhibitor. Our study is the first to use a specific genetic deletion of hepatocyte Abca1 and supports their conclusion. We also observed increased selective HDL ³H-CO removal from plasma in HSKO versus control mice, in agreement with two turnover studies using probucol inhibition in mice^{23, 48}. Decreased plasma HDL pool size is unlikely to explain the more rapid plasma decay of HDL ³H-CO in HSKO recipient mice, since low plasma HDL in apoA-I knockout mice did not affect plasma removal of HDL ³H-FC or ³H-CE⁴⁹. Further, normalization of the HDL pool in a Tangier disease subject by infusion of human HDL did not normalize rapid plasma decay of HDL⁵⁰. Our results demonstrate a novel role for hepatocyte Abca1 in regulating plasma HDL-C trafficking into the RCT pathway for fecal excretion, and suggest that loss or reduction of hepatocyte Abca1 activity might enhance net removal of cholesterol from the body.

The concept that hepatic Abca1 facilitates HDL-derived hepatic cholesterol resecretion into plasma, diverting it from RCT, was suggested by Yamamoto et al²³; however, *in vivo* support was lacking. Our study demonstrates that HSKO mice had reduced resecretion of plasma HDL-derived cholesterol, taken up by the liver, back into plasma and altered compartmentalization of cholesterol with a relative increase in VLDL FC secretion and a decrease in HDL FC and CE secretion (Fig. 4). To quantify hepatic resecretion of internalized plasma HDL-CE, two criteria must be met. First, HDL ³H-CO tracer must not undergo significant hydrolysis in plasma during the turnover study and second, ³H-CO must be significantly hydrolyzed after hepatic uptake to release ³H-FC for resecretion. Our control data demonstrate that these criteria were met (Supplemental Fig. I and II). Our previous study showed increased secretion of larger, TG-enriched VLDL particles in HSKO mice, hepatocytes from HSKO mice, and hepatoma cells with silenced Abca1^{18, 51, 52}, compatible with increased VLDL ³H-FC appearance in HSKO plasma 24 hours after HDL ³H-CO injection, relative to controls. This finding also agrees with results demonstrating that Abca1-stimulated FC efflux from hepatoma cells and primary hepatocytes decreases the pool of hepatocyte FC available for VLDL secretion⁵³. These data support an emerging concept that Abca1 is critical in affecting hepatic lipid (TG and FC) trafficking into several pathways, including biliary secretion for RCT, VLDL secretion, and HDL particle assembly.

We previously showed that HSKO mice in a mixed (80% C57Bl/6– 20% 129/SvEv) genetic background had significantly higher selective hepatic uptake of HDL CE than control mice, presumably via SR-BI, although hepatic SR-BI protein expression was similar between the two genotypes²¹. However, selective plasma removal of HDL ³H-CO in HSKO versus control mice in our current study seemed too high to be explained by SR-BI expression alone. For example, hepatic-specific SR-BI transgenic mice, exhibiting 12-fold overexpression of mouse SR-BI, had a 2-fold increase in selective HDL CE removal from plasma⁵⁴, less than the 4-fold increase in plasma HDL-CE selective removal in HSKO mice, relative to control (Fig. 2C). Furthermore, we observed a significant *decrease*, not increase, in hepatic SR-BI protein expression in HSKO mice compared to controls across several

cohorts. We verified that SR-BI protein expression, but not mRNA abundance, was significantly decreased in another cohort of HSKO relative to control mice (n=5/group; data not shown; 48-hour macrophage RCT study). The difference in liver SR-BI expression compared to our past study²¹ may relate to our use of HSKO and control mice that were >99% in the C57Bl/6 background¹⁸. These combined results suggested another explanation besides SR-BI expression for the more rapid selective removal of plasma HDL ³H-CO in HSKO mice.

In our previous study, liver LDLr expression was increased ~2-fold in HSKO mice versus controls, resulting in increased plasma ¹²⁵I-LDL turnover¹⁸. This magnitude of LDLr overexpression is associated with significantly reduced plasma HDL-C concentrations in other mouse models^{43,44}. We tested the hypothesis that higher LDLr expression in HSKO liver increased plasma HDL ³H-CO removal, compared to control mice, but found no difference in hepatic LDLr expression. In other unpublished studies, we have observed significantly increased hepatic LDLr protein expression and mRNA abundance in HSKO versus control mice after a 24-hour fast. Recipient mice in the current study were not fasted before sacrifice after 24- or 48-hour turnover studies. Whether the physiologic extremes of fasting and fasting-refeeding result in a unique regulation of hepatic LDLr expression in HSKO mice requires further investigation.

Despite similar hepatic LDLr expression in HSKO and control mice in this study, hepatic LDLr silencing normalized rapid removal of HDL ³H-CO from plasma, selective plasma HDL ³H-CO removal, and RCT in HSKO mice to those of control mice (Fig. 7). Similar, but less striking, trends were observed with control mice treated with LDLr ASO versus control ASO, in general agreement with results of Rinninger et al⁵⁵, who demonstrated that plasma HDL CE selective removal and hepatic selective uptake of HDL CE were nearly eliminated in LDLr knockout mice versus wild-type controls. HSKO mice treated with LDLr ASO had similar hepatic ³H radiolabel accumulation as HSKO mice treated with control ASO, but the former had decreased fecal ³H radiolabel (Fig. 7D-E), suggesting that hepatic LDLr may also play a role in intrahepatic FC trafficking into bile and feces, resulting in diminished fecal ³H radiolabel when the LDLr is silenced. We speculate that there may be greater hepatocyte LDLr surface expression or faster endocytic recycling back to the plasma membrane in HSKO mice to explain the dependence of increased HDL catabolism on hepatic LDLr expression.

One perplexing observation is why macrophage RCT is not decreased when hepatocyte Abca1 is absent (Fig. 8). We previously demonstrated that macrophage RCT was not compromised in atherogenic diet-fed, hyperlipidemic HSKO/LDLr double knockout mice versus controls (i.e., LDLrKO), suggesting hepatic Abca1 deletion has no impact on macrophage RCT³⁶. Our current study shows this outcome was unrelated to hyperlipidemic background or atherogenic diet feeding. Our results agree with those of Yamamoto et al²³, who showed that macrophage RCT was not stimulated in probucol-fed mice although plasma HDL CE RCT was increased versus controls. One possible explanation is that not all radiolabeled cholesterol in macrophages used for RCT studies is esterified and RCT for macrophage ³H-FC may be more efficient than ³H-CE, which must first be hydrolyzed to ³H-FC before it can be effluxed from macrophages. A small, dynamic HDL pool, such as

pre- β 1 HDL⁵⁶, may efficiently remove excess macrophage ³H-FC, which is quantitatively insignificant relative to the mass of cholesterol in plasma, and rapidly transport it to the liver for excretion without a detectable increase in plasma HDL-C. Another potential explanation is that red blood cells become quantitatively more important for macrophage RCT in low plasma HDL situations, such as HSKO and apoA-I knockout mice⁵⁷. Finally, although much attention has been focused on macrophage Abca1 in RCT, our study clearly documents a critical role for hepatocyte Abca1 in hepatic FC trafficking and plasma HDL RCT.

Supplementary Material

Refer to Web version on PubMed Central for supplementary material.

Acknowledgments:

The authors gratefully acknowledge Abraham K. Gebre for technical assistance and Dr. Joachim Herz, University of Texas, Southwestern, for providing anti-mouse LDLr antiserum. We also acknowledge the editorial assistance of Karen Klein, MA, in the Wake Forest Clinical and Translational Science Institute (UL1 TR001420; PI: McClain).

Sources of funding: This project was supported by funding from the National Institutes of Health R01 HL119962 (to J.S.P.) and T32 HL091797 (A.C.B.)

Non-standard Abbreviations and Acronyms:

Abca1	ATP binding cassette transport A1
FC	Free cholesterol
HDL	High density lipoprotein
HDL-C	High density lipoprotein cholesterol
RCT	Reverse cholesterol transport
HSKO	Hepatocyte-specific Abca1 knockout
CO	Cholesteryl oleate
CE	Cholesteryl ester
VLDL	Very low density lipoprotein
SR-BI	Scavenger receptor class B type 1
LDLr	Low density lipoprotein receptor
CHD	Coronary heart disease
LDL	Low density lipoprotein
ASO	Antisense oligonucleotide
TC	Tyramine cellobiose

LPDS	Lipoprotein-deficient serum
FPLC	Fast protein liquid chromatography
HPLC	High performance liquid chromatography
TBST	Tris-buffered saline + 1% tween 20
TPC	Total plasma cholesterol
FCR	Fractional catabolic rate

References

1. Singh IM, Shishehbor MH, Ansell BJ. High-density lipoprotein as a therapeutic target: A systematic review. *JAMA*. 2007;298:786–798 [PubMed: 17699012]
2. Baigent C, Keech A, Kearney PM, Blackwell L, Buck G, Pollicino C, Kirby A, Sourjina T, Peto R, Collins R, Simes R, Cholesterol Treatment Trialists C. Efficacy and safety of cholesterol-lowering treatment: Prospective meta-analysis of data from 90,056 participants in 14 randomised trials of statins. *Lancet*. 2005;366:1267–1278 [PubMed: 16214597]
3. Miller GJ, Miller NE. Plasma-high-density-lipoprotein concentration and development of ischaemic heart-disease. *Lancet*. 1975;1:16–19 [PubMed: 46338]
4. Castelli WP, Doyle JT, Gordon T, Hames CG, Hjortland MC, Hulley SB, Kagan A, Zukel WJ. Hdl cholesterol and other lipids in coronary heart disease. The cooperative lipoprotein phenotyping study. *Circulation*. 1977;55:767–772 [PubMed: 191215]
5. Miller NE, Thelle DS, Forde OH, Mjos OD. The Tromso heart-study. High-density lipoprotein and coronary heart-disease: A prospective case-control study. *Lancet*. 1977;1:965–968 [PubMed: 67464]
6. Barter PJ, Caulfield M, Eriksson M, Grundy SM, Kastelein JJ, Komajda M, Lopez-Sendon J, Mosca L, Tardif JC, Waters DD, Shear CL, Revkin JH, Buhr KA, Fisher MR, Tall AR, Brewer B, Investigators I. Effects of torcetrapib in patients at high risk for coronary events. *N. Engl. J. Med* 2007;357:2109–2122 [PubMed: 17984165]
7. Schwartz GG, Olsson AG, Abt M, Ballantyne CM, Barter PJ, Brumm J, Chaitman BR, Holme IM, Kallend D, Leiter LA, Leitersdorf E, McMurray JJ, Mundl H, Nicholls SJ, Shah PK, Tardif JC, Wright RS, dal OI. Effects of dalcetrapib in patients with a recent acute coronary syndrome. *N. Engl. J. Med* 2012;367:2089–2099 [PubMed: 23126252]
8. Investigators A-H, Boden WE, Probstfield JL, Anderson T, Chaitman BR, Desvignes-Nickens P, Koprowicz K, McBride R, Teo K, Weintraub W. Niacin in patients with low hdl cholesterol levels receiving intensive statin therapy. *N. Engl. J. Med* 2011;365:2255–2267 [PubMed: 22085343]
9. Lewis GF, Rader DJ. New insights into the regulation of hdl metabolism and reverse cholesterol transport. *Circulation Res*. 2005;96:1221–1232 [PubMed: 15976321]
10. Khera AV, Cuchel M, de la Llera-Moya M, Rodrigues A, Burke MF, Jafri K, French BC, Phillips JA, Mucksavage ML, Wilensky RL, Mohler ER, Rothblat GH, Rader DJ. Cholesterol efflux capacity, high-density lipoprotein function, and atherosclerosis. *N. Engl. J. Med* 2011;364:127–135 [PubMed: 21226578]
11. Rohatgi A, Khera A, Berry JD, Givens EG, Ayers CR, Wedin KE, Neeland IJ, Yuhanna IS, Rader DR, de Lemos JA, Shaul PW. Hdl cholesterol efflux capacity and incident cardiovascular events. *N. Engl. J. Med* 2014;371:2383–2393 [PubMed: 25404125]
12. Francis GA. The complexity of hdl. *Biochim Biophys Acta*. 2010;1801:1286–1293 [PubMed: 20736082]
13. Oram JF, Heinecke JW. ATP-binding cassette transporter a1: A cell cholesterol exporter that protects against cardiovascular disease. *Physiol. Rev*. 2005;85:1343–1372 [PubMed: 16183915]
14. Timmins JM, Lee JY, Boudyguina E, Kluckman KD, Brunham LR, Mulya A, Gebre AK, Coutinho JM, Colvin PL, Smith TL, Hayden MR, Maeda N, Parks JS. Targeted inactivation of hepatic abca1

- causes profound hypoalphalipoproteinemia and kidney hypercatabolism of apoA-I. *J. Clin. Invest* 2005;115:1333–1342 [PubMed: 15841208]
15. Bodzioch M, Orso E, Klucken J, Langmann T, Bottcher A, Diederich W, Drobnik W, Barlage S, Buchler C, Porsch-Ozcuremez M, Kaminski WE, Hahmann HW, Oette K, Rothe G, Aslanidis C, Lackner KJ, Schmitz G. The gene encoding atp-binding cassette transporter 1 is mutated in tangier disease. *Nat. Genet* 1999;22:347–351 [PubMed: 10431237]
 16. Rust S, Rosier M, Funke H, Real J, Amoura Z, Piette JC, Deleuze JF, Brewer HB, Duverger N, Deneffe P, Assmann G. Tangier disease is caused by mutations in the gene encoding atp-binding cassette transporter 1. *Nat. Genet* 1999;22:352–355 [PubMed: 10431238]
 17. Brooks-Wilson A, Marcil M, Clee SM, Zhang LH, Roomp K, van Dam M, Yu L, Brewer C, Collins JA, Molhuizen HO, Loubser O, Ouellette BF, Fichter K, Ashbourne-Excoffon KJ, Sensen CW, Scherer S, Mott S, Denis M, Martindale D, Frohlich J, Morgan K, Koop B, Pimstone S, Kastelein JJ, Genest J, Jr., Hayden MR. Mutations in *abcl1* in tangier disease and familial high-density lipoprotein deficiency. *Nat. Genet* 1999;22:336–345 [PubMed: 10431236]
 18. Chung S, Timmins JM, Duong M, Degirolamo C, Rong S, Sawyer JK, Singaraja RR, Hayden MR, Maeda N, Rudel LL, Shelness GS, Parks JS. Targeted deletion of hepatocyte *abca1* leads to very low density lipoprotein triglyceride overproduction and low density lipoprotein hypercatabolism. *J. Biol. Chem* 2010;285:12197–12209 [PubMed: 20178985]
 19. Brunham LR, Kruit JK, Iqbal J, Fievet C, Timmins JM, Pape TD, Coburn BA, Bissada N, Staels B, Groen AK, Hussain MM, Parks JS, Kuipers F, Hayden MR. Intestinal *abca1* directly contributes to hdl biogenesis in vivo. *J. Clin. Invest* 2006;116:1052–1062 [PubMed: 16543947]
 20. Chung S, Sawyer JK, Gebre AK, Maeda N, Parks JS. Adipose tissue atp binding cassette transporter 1 contributes to high-density lipoprotein biogenesis in vivo. *Circulation*. 2011;124:1663–1672 [PubMed: 21931081]
 21. Singaraja RR, Stahmer B, Brundert M, Merkel M, Heeren J, Bissada N, Kang M, Timmins JM, Ramakrishnan R, Parks JS, Hayden MR, Rinninger F. Hepatic atp-binding cassette transporter 1 is a key molecule in high-density lipoprotein cholesteryl ester metabolism in mice. *Arterioscler. Thromb. Vasc. Biol* 2006;26:1821–1827 [PubMed: 16728652]
 22. Liu M, Chung S, Shelness GS, Parks JS. Hepatic *abca1* and vldl triglyceride production. *Biochim. Biophys. Acta* 2012;1821:770–777 [PubMed: 22001232]
 23. Yamamoto S, Tanigawa H, Li X, Komaru Y, Billheimer JT, Rader DJ. Pharmacologic suppression of hepatic atp-binding cassette transporter 1 activity in mice reduces high-density lipoprotein cholesterol levels but promotes reverse cholesterol transport. *Circulation*. 2011;124:1382–1390 [PubMed: 21859969]
 24. Yamashita S, Masuda D, Matsuzawa Y. Did we abandon probucol too soon? *Curr. Opin. Lipidol* 2015;26:304–316 [PubMed: 26125504]
 25. Yamashita S, Matsuzawa Y. Where are we with probucol: A new life for an old drug? *Atherosclerosis*. 2009;207:16–23 [PubMed: 19457483]
 26. Havel RJ, Eder HA, Bragdon JH. The distribution and chemical composition of ultracentrifugally separated lipoproteins in human serum. *J Clin Invest*. 1955;34:1345–1353 [PubMed: 13252080]
 27. Terpstra AH, Nicolosi RJ, Herbert PN. In vitro incorporation of radiolabeled cholesteryl esters into high and low density lipoproteins. *J. Lipid Res*. 1989;30:1663–1671 [PubMed: 2693568]
 28. Pittman RC, Carew TE, Glass CK, Green SR, Taylor CA Jr., Attie AD. A radioiodinated, intracellularly trapped ligand for determining the sites of plasma protein degradation in vivo. *Biochem. J*. 1983;212:791–800 [PubMed: 6882394]
 29. Lee JY, Lanningham-Foster L, Boudyguina EY, Smith TL, Young ER, Colvin PL, Thomas MJ, Parks JS. Prebeta high density lipoprotein has two metabolic fates in human apolipoprotein a-i transgenic mice. *J Lipid Res*. 2004;45:716–728 [PubMed: 14729861]
 30. Bligh EG, Dyer WJ. A rapid method of total lipid extraction and purification. *Can J Biochem Physiol*. 1959;37:911–917 [PubMed: 13671378]
 31. Parks JS, Rudel LL. Metabolism of the serum amyloid A proteins (*ssa*) in high-density lipoproteins and chylomicrons of nonhuman primates (vervet monkey). *Am J Pathol*. 1983;112:243–249 [PubMed: 6412556]

32. Folch J, Lees M, Sloane Stanley GH. A simple method for the isolation and purification of total lipides from animal tissues. *J. Biol. Chem* 1957;226:497–509 [PubMed: 13428781]
33. Temel RE, Sawyer JK, Yu L, Lord C, Degirolamo C, McDaniel A, Marshall S, Wang N, Shah R, Rudel LL, Brown JM. Biliary sterol secretion is not required for macrophage reverse cholesterol transport. *Cell Metab.* 2010;12:96–102 [PubMed: 20620999]
34. Varban ML, Rinninger F, Wang N, Fairchild-Huntress V, Dunmore JH, Fang Q, Gosselin ML, Dixon KL, Deeds JD, Acton SL, Tall AR, Huszar D. Targeted mutation reveals a central role for sr-bi in hepatic selective uptake of high density lipoprotein cholesterol. *Proc Natl Acad Sci U S A.* 1998;95:4619–4624 [PubMed: 9539787]
35. Thomas MS, Rudel LL. Intravascular metabolism of lipoprotein cholesteryl esters in african green monkeys: Differential fate of doubly labeled cholesteryl oleate. *J. Lipid Res.* 1987;28:572–581 [PubMed: 3598399]
36. Bi X, Zhu X, Duong M, Boudyguina EY, Wilson MD, Gebre AK, Parks JS. Liver abca1 deletion in ldlrko mice does not impair macrophage reverse cholesterol transport or exacerbate atherogenesis. *Arterioscler. Thromb. Vasc. Biol* 2013;33:2288–2296 [PubMed: 23814116]
37. Allain CC, Poon LS, Chan CS, Richmond W, Fu PC. Enzymatic determination of total serum cholesterol. *Clinical chemistry.* 1974;20:470–475 [PubMed: 4818200]
38. Livak KJ, Schmittgen TD. Analysis of relative gene expression data using real-time quantitative pcr and the 2(-delta delta c(t)) method. *Methods.* 2001;25:402–408 [PubMed: 11846609]
39. Lee JY, Timmins JM, Mulya A, Smith TL, Zhu Y, Rubin EM, Chisholm JW, Colvin PL, Parks JS. Hdl in apo-a-i transgenic abca1 knockout mice are remodeled normally in plasma but are hypercatabolized by the kidney. *J. Lipid Res* 2005;46:2233–2245 [PubMed: 16024913]
40. Blanche PJ, Gong EL, Forte TM, Nichols AV. Characterization of human high-density lipoproteins by gradient gel electrophoresis. *Biochim Biophys Acta.* 1981;665:408–419 [PubMed: 7295744]
41. Huggins KW, Bureson ER, Sawyer JK, Kelly K, Rudel LL, Parks JS. Determination of the tissue sites responsible for the catabolism of large high density lipoprotein in the african green monkey. *J. Lipid Res* 2000;41:384–394 [PubMed: 10706586]
42. Acton S, Rigotti A, Landschulz KT, Xu S, Hobbs HH, Krieger M. Identification of scavenger receptor sr-bi as a high density lipoprotein receptor. *Science.* 1996;271:518–520 [PubMed: 8560269]
43. Knouff C, Malloy S, Wilder J, Altenburg MK, Maeda N. Doubling expression of the low density lipoprotein receptor by truncation of the 3'-untranslated region sequence ameliorates type iii hyperlipoproteinemia in mice expressing the human apoe2 isoform. *J. Biol. Chem* 2001;276:3856–3862 [PubMed: 11076954]
44. Rashid S, Curtis DE, Garuti R, Anderson NN, Bashmakov Y, Ho YK, Hammer RE, Moon YA, Horton JD. Decreased plasma cholesterol and hypersensitivity to statins in mice lacking pcsk9. *Proc. Natl. Acad. Sci. U. S. A* 2005;102:5374–5379 [PubMed: 15805190]
45. Groen AK, Bloks VW, Bandsma RH, Ottenhoff R, Chimini G, Kuipers F. Hepatobiliary cholesterol transport is not impaired in abca1-null mice lacking hdl. *J. Clin. Invest* 2001;108:843–850 [PubMed: 11560953]
46. Drobnik W, Lindenthal B, Lieser B, Ritter M, Christiansen Weber T, Liebisch G, Giesa U, Igel M, Borsukova H, Buchler C, Fung-Leung WP, Von Bergmann K, Schmitz G. Atp-binding cassette transporter a1 (abca1) affects total body sterol metabolism. *Gastroenterology.* 2001;120:1203–1211 [PubMed: 11266384]
47. Wellington CL, Walker EK, Suarez A, Kwok A, Bissada N, Singaraja R, Yang YZ, Zhang LH, James E, Wilson JE, Francone O, McManus BM, Hayden MR. Abca1 mrna and protein distribution patterns predict multiple different roles and levels of regulation. *Lab. Invest* 2002;82:273–283 [PubMed: 11896206]
48. Rinninger F, Wang N, Ramakrishnan R, Jiang XC, Tall AR. Probucol enhances selective uptake of hdl-associated cholesteryl esters in vitro by a scavenger receptor b-i-dependent mechanism. *Arterioscler. Thromb. Vasc. Biol* 1999;19:1325–1332 [PubMed: 10323786]
49. Ji Y, Wang N, Ramakrishnan R, Sehayek E, Huszar D, Breslow JL, Tall AR. Hepatic scavenger receptor bi promotes rapid clearance of high density lipoprotein free cholesterol and its transport into bile. *J. Biol. Chem* 1999;274:33398–33402 [PubMed: 10559220]

50. Schaefer EJ, Blum CB, Levy RI, Jenkins LL, Alaupovic P, Foster DM, Brewer HB, Jr. Metabolism of high-density lipoprotein apolipoproteins in tangier disease. *N. Engl. J. Med* 1978;299:905–910 [PubMed: 211412]
51. Chung S, Gebre AK, Seo J, Shelness GS, Parks JS. A novel role for abca1-generated large pre-beta migrating nascent hdl in the regulation of hepatic vldl triglyceride secretion. *J. Lipid Res* 2010;51:729–742 [PubMed: 20215580]
52. Liu M, Chung S, Shelness GS, Parks JS. Hepatic abca1 deficiency is associated with delayed apolipoprotein b secretory trafficking and augmented vldl triglyceride secretion. *Biochim. Biophys. Acta* 2017;1862:1035–1043
53. Sahoo D, Trischuk TC, Chan T, Drover VA, Ho S, Chimini G, Agellon LB, Agnihotri R, Francis GA, Lehner R. Abca1-dependent lipid efflux to apolipoprotein a-i mediates hdl particle formation and decreases vldl secretion from murine hepatocytes. *J. Lipid Res* 2004;45:1122–1131 [PubMed: 14993246]
54. Wang N, Arai T, Ji Y, Rinninger F, Tall AR. Liver-specific overexpression of scavenger receptor bi decreases levels of very low density lipoprotein apob, low density lipoprotein apob, and high density lipoprotein in transgenic mice. *J. Biol. Chem* 1998;273:32920–32926 [PubMed: 9830042]
55. Rinninger F, Heine M, Singaraja R, Hayden M, Brundert M, Ramakrishnan R, Heeren J. High density lipoprotein metabolism in low density lipoprotein receptor-deficient mice. *J. Lipid Res* 2014;55:1914–1924 [PubMed: 24954421]
56. de la Llera-Moya M, Drazul-Schrader D, Asztalos BF, Cuchel M, Rader DJ, Rothblat GH. The ability to promote efflux via abca1 determines the capacity of serum specimens with similar high-density lipoprotein cholesterol to remove cholesterol from macrophages. *Arterioscler. Thromb. Vasc. Biol* 2010;30:796–801 [PubMed: 20075420]
57. Hung KT, Berisha SZ, Ritchey BM, Santore J, Smith JD. Red blood cells play a role in reverse cholesterol transport. *Arterioscler. Thromb. Vasc. Biol* 2012;32:1460–1465 [PubMed: 22499994]

Highlights

- Plasma HDL CE clearance is increased in the absence of hepatic Abca1, contributing to reduced plasma HDL cholesterol concentrations
- Increased plasma HDL CE clearance in mice lacking hepatocyte Abca1 requires hepatic LDL receptor expression
- In the absence of hepatocyte Abca1, less plasma HDL-derived hepatic FC is recycled back into plasma as nascent HDL and a relatively greater proportion of HDL-derived hepatic FC is secreted from liver in VLDL particles
- Reverse cholesterol transport of plasma HDL cholesterol into feces is increased in mice lacking hepatocyte Abca1

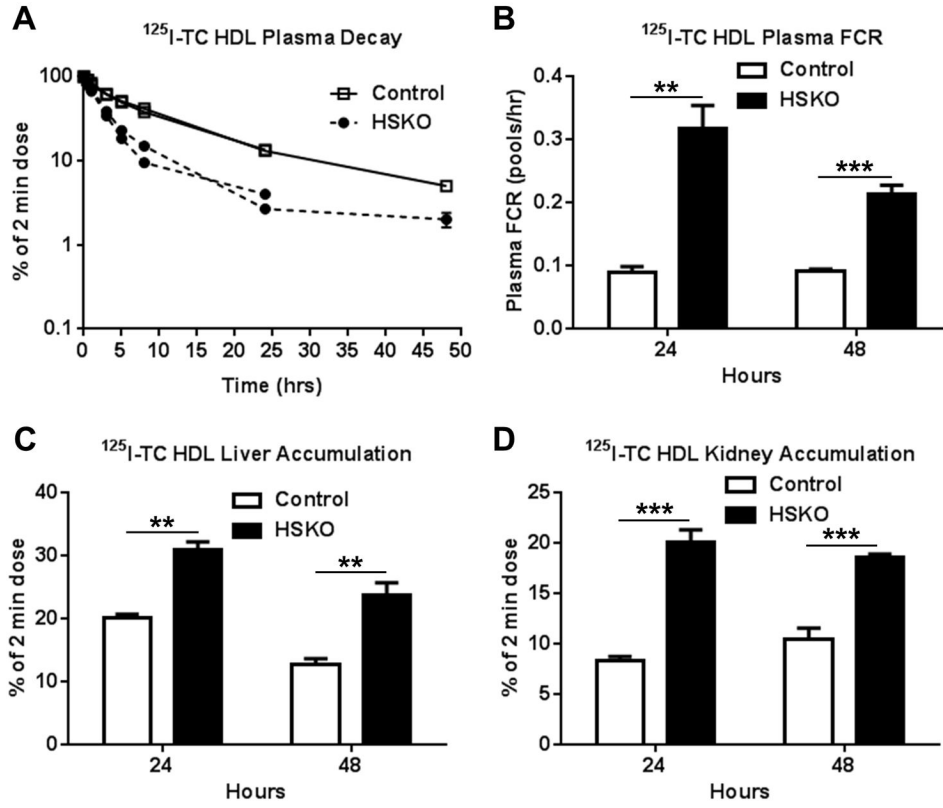


Figure 1. *In vivo* catabolism of ¹²⁵I-TC radiolabeled human HDL. ¹²⁵I-TC radiolabeled human HDL was injected intravenously into chow-fed control (n=6) and HSKO (n=6) mice in two separate turnover studies lasting 24 or 48 hours. Periodic blood samples were taken over 24 or 48 hours to analyze plasma decay (A), plasma FCR (B), liver (C), and kidney accumulation (D) of the ¹²⁵I-TC tracer. Data are mean ± SEM. Control turnover curves in panel A are nearly identical and SEM in nearly all points falls within the symbol. **p < 0.01; ***p < 0.001.

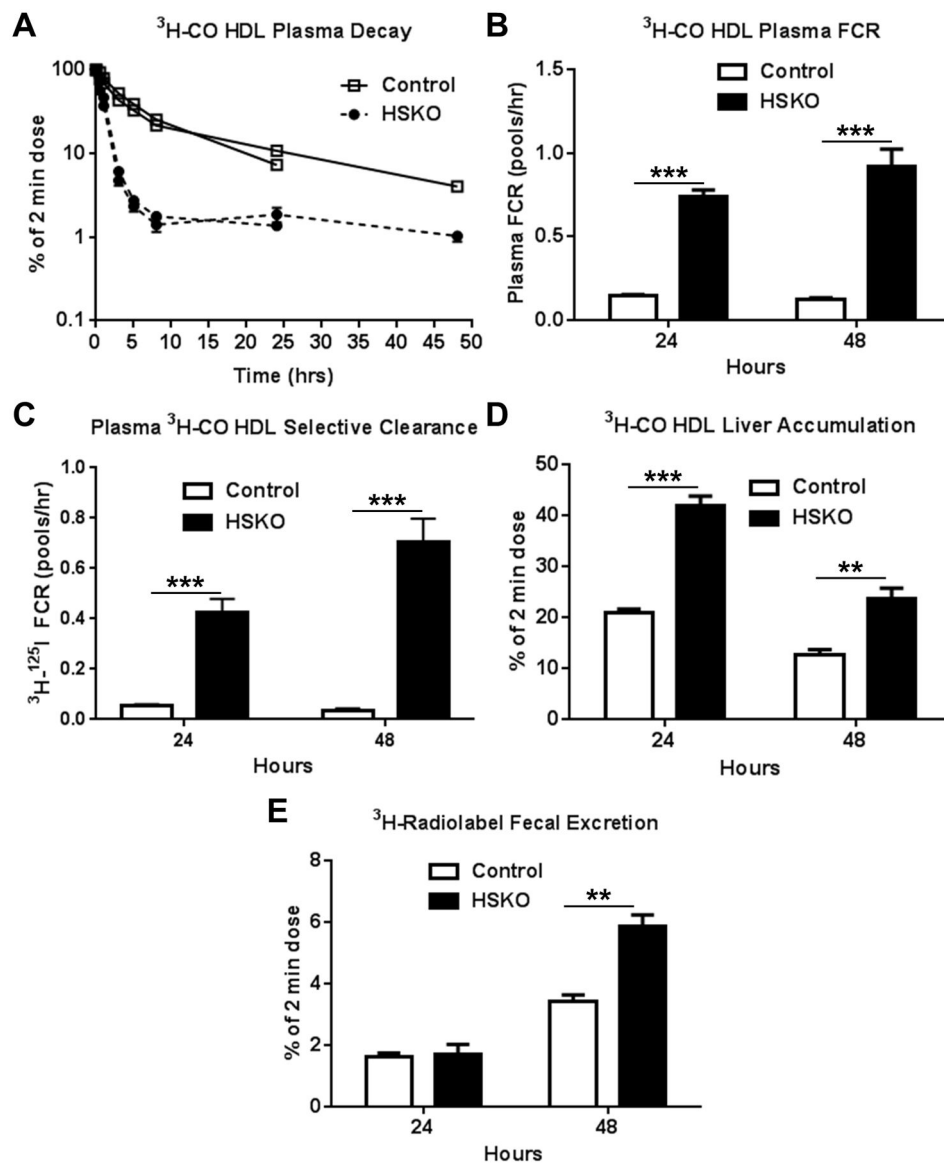


Figure 2. *In vivo* catabolism and RCT of plasma HDL CO. $^3\text{H-CO}$ radiolabeled human HDL was injected intravenously in control (n=6) and HSKO (n=6) mice with $^{125}\text{I-TC}$ HDL (see Figure 1). Periodic blood samples were taken over 24 or 48 hours in two separate experiments to analyze plasma decay (A), plasma FCR (B), plasma HDL $^3\text{H-CO}$ selective clearance, using data from Figure 1B for $^{125}\text{I-TC}$ FCR (C), liver ^3H -radiolabel accumulation (D), and fecal ^3H -radiolabel excretion (E). Data are mean \pm SEM. Control turnover curves in panel A are nearly identical and SEM in nearly all points falls within the symbol. **p < 0.01; ***p < 0.001.

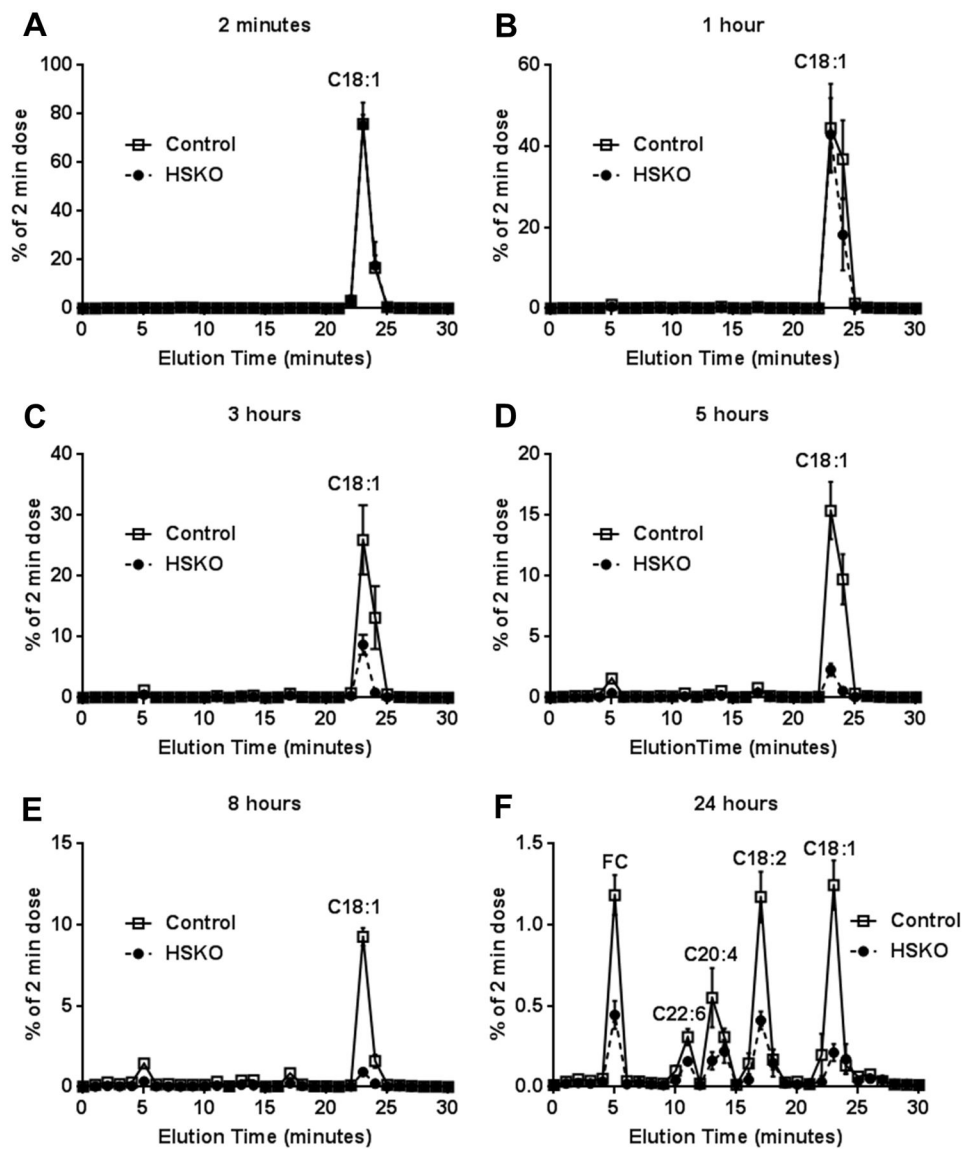


Figure 3. Resecretion of HDL-C into plasma. ^3H -CO-radiolabeled HDL was injected intravenously into control (n=5) and HSKO (n=5) mice. Periodic blood samples (A-F) were taken over 24 hours to trace disappearance of cholesterol oleate (C18:1) and reappearance of free cholesterol (FC), cholesteryl docosahexanoate (C22:6), cholesteryl arachidonate (C20:4), and cholesteryl linoleate (C18:2) in plasma by reverse phase HPLC. Each data point is the mean \pm SEM.

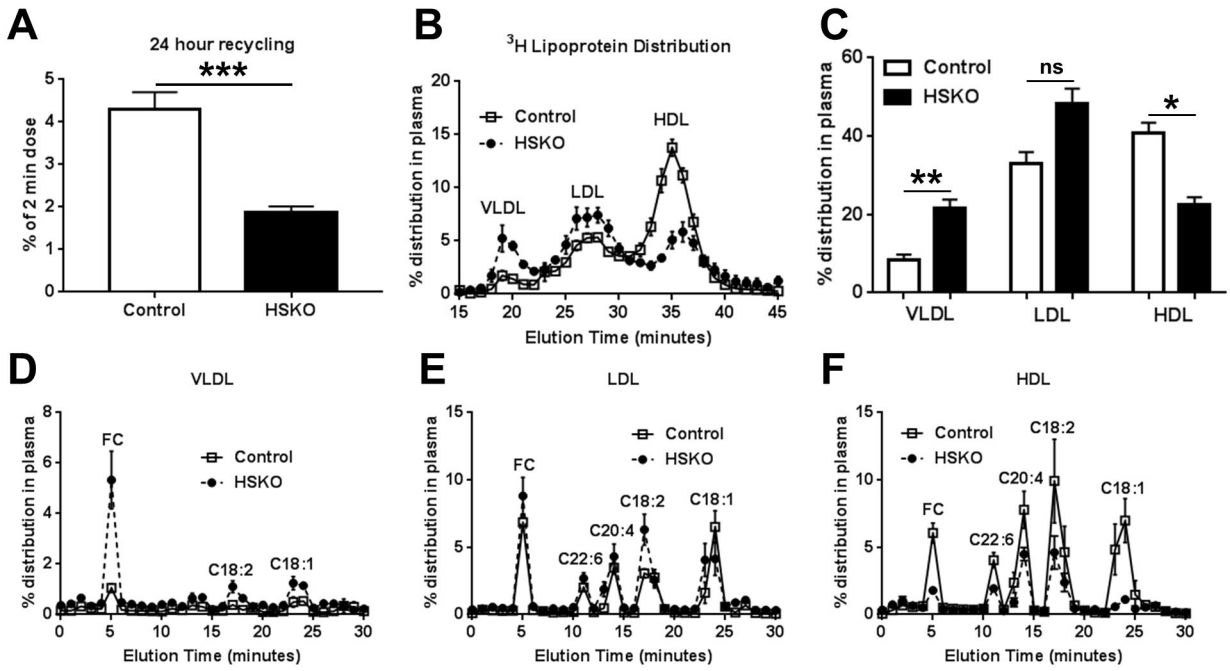


Figure 4. Plasma lipoprotein ^3H radiolabel distribution 24 hours after injection of ^3H -CO radiolabeled human HDL. Total ^3H -CO HDL radiolabel removed by the liver and recycled into plasma at 24 hours was calculated as the sum of radiolabel in fractions 0-20 from Figure 3F (i.e., ^3H -FC + ^3H -CE radioactivity exclusive of ^3H -C18:1) (A). Plasma isolated from 24-hour terminal blood samples was fractionated by FPLC and percentage radiolabel distribution in each lipoprotein fraction was plotted (B). ^3H -radiolabel percentage distribution in panel B, calculated as area under the curve from FPLC profiles (C). VLDL, LDL, and HDL FPLC fractions (i.e., panel B) were pooled, lipid extracted, FC and CE fatty acyl species fractionated by HPLC, and radiolabeled ^3H -FC and ^3H -CE fatty acyl species in VLDL (D), LDL (E), and HDL (F) quantified by liquid scintillation counting. Data are mean \pm SEM; n=5/genotype. *p < 0.05; **p < 0.01; ***p < 0.001.

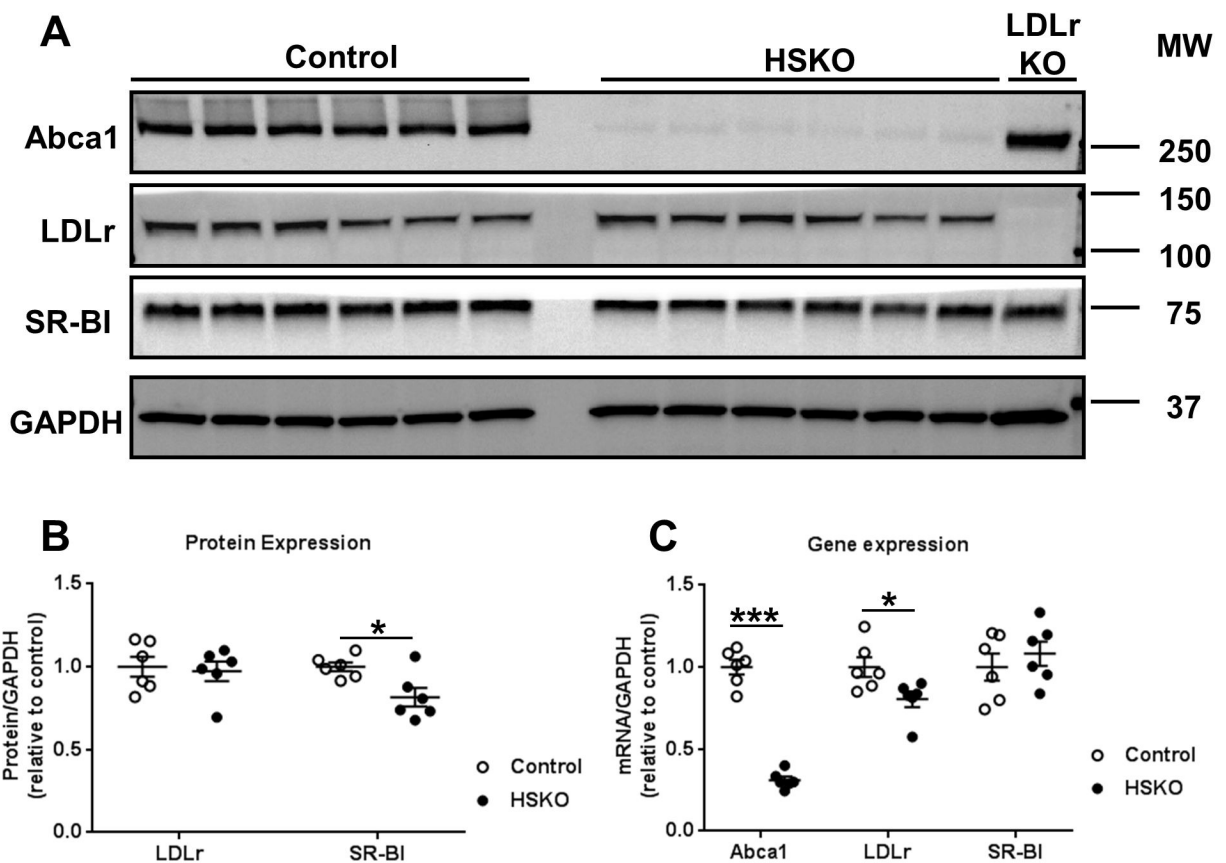


Figure 5.

Hepatic Abca1, LDLr, and SR-BI protein expression and gene expression. Whole liver lysates from control (n=6) and HSKO (n=6) were immunoblotted for Abca1, LDLr, SR-BI, and GAPDH, as loading control (A). Immunoblots in panel A for LDLr and SR-BI were quantified by calculating fold change of the protein/GAPDH ratio relative to control livers (B). Abca1, LDLr, and SR-BI gene expression was analyzed by real-time PCR and the mRNA/GAPDH ratio relative to control livers was quantified (C). Data are mean \pm SEM; n=6/genotype from recipient mice used for the 24-hour turnover study in figures 1 and 2. *p < 0.05; ***p < 0.001.

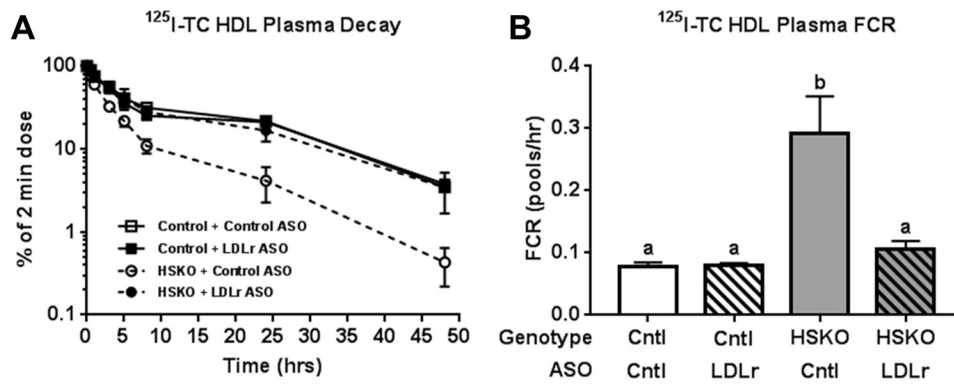


Figure 6. Effect of LDLr ASO treatment on *in vivo* catabolism of ¹²⁵I-TC radiolabeled human HDL. ¹²⁵I-TC radiolabeled HDL was injected intravenously into control and HSKO mice treated with a control (Cntl) or LDLr-targeting ASO. Periodic blood samples were taken over 48 hours to analyze plasma decay (A) and FCR (B). Data are mean ± SEM. Groups with different letters are statistically different (p<0.05), n=3/group.

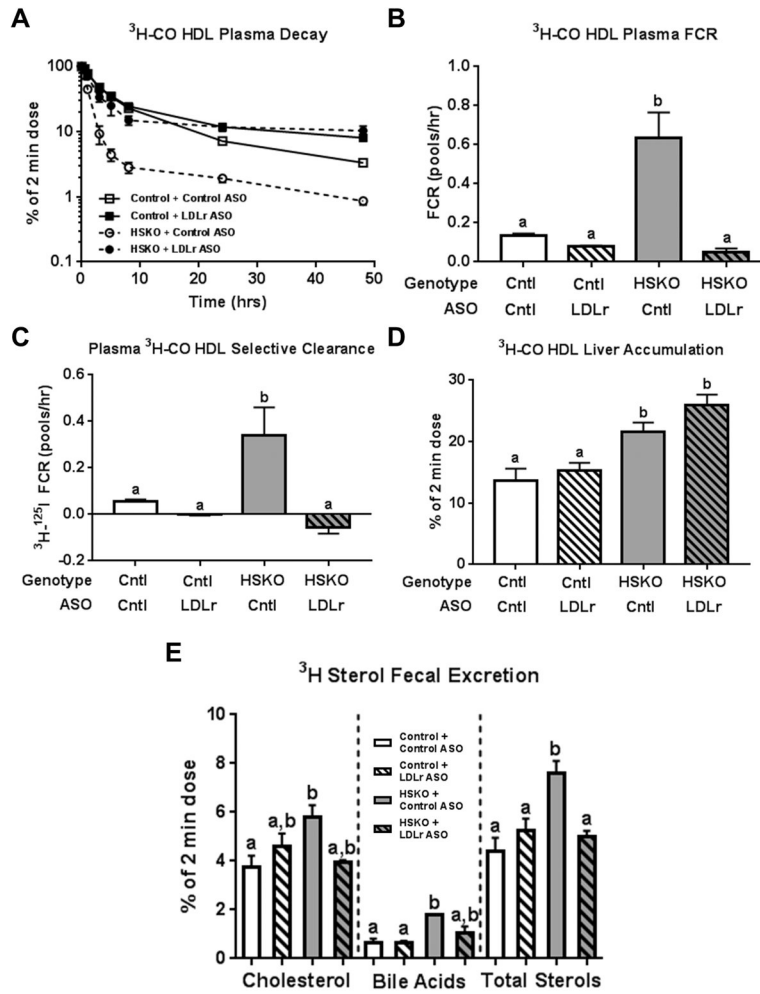


Figure 7. Effect of LDLr ASO treatment on *in vivo* catabolism of ³H-CO radiolabeled human HDL. ³H-CO-radiolabeled HDL was injected intravenously in control and HSKO mice treated with a control or LDLr targeting ASO. Periodic blood samples were taken over 48 hours to analyze plasma decay (A), plasma FCR (B), and plasma HDL ³H-CO selective clearance, using data from Figure 7B for ¹²⁵I-TC FCR (C). Tissues were then harvested to quantify liver accumulation (D) and fecal excretion (E) of the ³H-tracer as bile acid, cholesterol or total sterol (bile acids + cholesterol). Data are mean ± SEM. Groups with different letters are statistically different (p<0.05), n=3/group. Data in panel B were analyzed with the Kruskal-Wallis non-parametric ANOVA (p=0.0001), followed by Dunn’s multiple comparisons test.

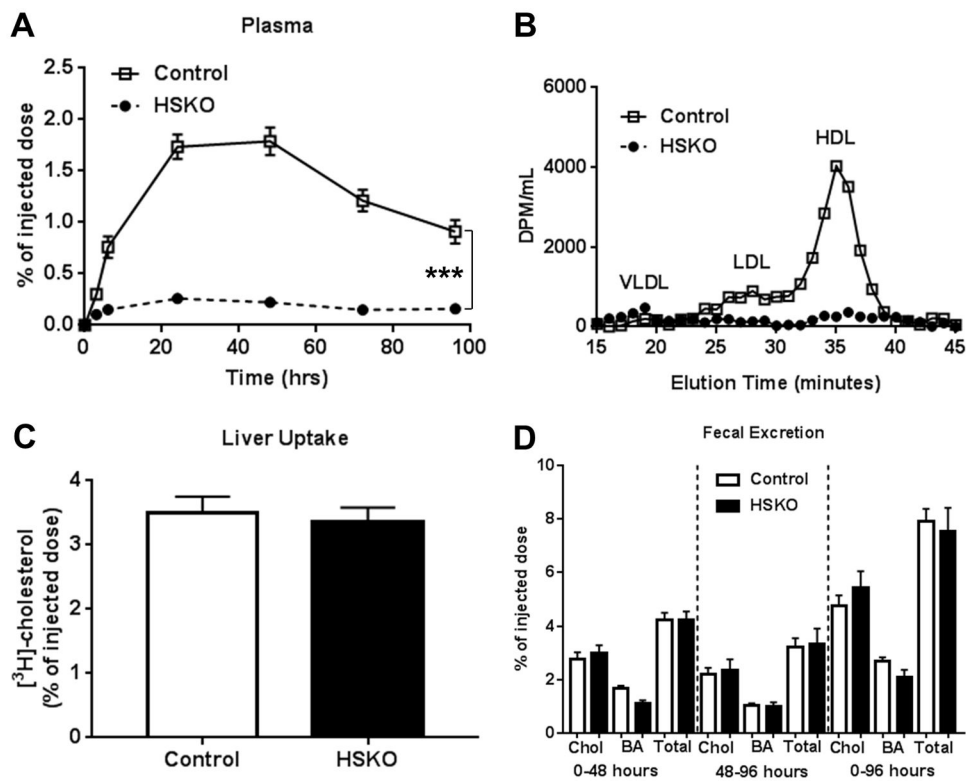


Figure 8. Macrophage reverse cholesterol transport. Control (n=6) and HSKO (n=6) mice were injected intraperitoneally with ³H-cholesterol-loaded J774 macrophages. Blood samples were taken over 96 hours to monitor plasma appearance of ³H-radiolabel (A). 48-hour plasma samples were fractionated by FPLC to determine ³H-radiolabeled lipoprotein distribution (B). At 96 hours, mice were sacrificed and liver ³H radiolabel uptake was measured (C). Feces were collected from 0-48 hours and 48-96h and ³H-radiolabeled cholesterol (Chol) and bile acid (BA) excretion were quantified (D). Total sterol ³H-radiolabel = Chol + BA radiolabel. Data are mean ± SEM.